applied sciences

MDPI

Article

Stability Analysis and Instability Time Prediction of Tunnel Roofs in a Karst Region Based on Catastrophe Theory

Yang Zou, Qianlong Tang * and Limin Peng

School of Civil Engineering, Central South University, Changsha 410075, China; 184801013@csu.edu.cn (Y.Z.); lmpeng@csu.edu.cn (L.P.)
* Correspondence: qlong21@126.com

Abstract: In order to address the safety construction issues of tunnels in karst areas, this study investigated the stability and instability time prediction of the roof of karst tunnels based on catastrophe theory. By establishing a discrimination equation for the sudden instability of the tunnel roof arch based on the elastic beam model and considering factors such as the self-weight of surrounding rocks and the position of caves, the calculation formula for the safety thickness of the roof of the karst tunnel was obtained. The study analyzed the impact of relevant factors on the safety thickness of the roof. Furthermore, a new method for predicting the instability of the tunnel roof arch was proposed, and it was validated through engineering examples. The results indicate that the water pressure in caves, the size of caves, the elasticity modulus of surrounding rocks, and the position of caves have extremely adverse effects on the safety of the arch roof. The calculation formula for the safety thickness of the roof of the karst tunnel derived from the theory of sudden change demonstrates feasibility and high accuracy in practical engineering applications. The established model for predicting roof instability can effectively forecast the time of roof arch instability in karst tunnels.

Keywords: karst tunnel; cusp catastrophe model; safety thickness; stability; instable time prediction

Academic Editor: Tiago Filipe da Silva Miranda

Received: 19 December 2024
Revised: 15 January 2025
Accepted: 16 January 2025
Published: 20 January 2025

Citation: Zou, Y.; Tang, Q.; Peng, L. Stability Analysis and Instability Time Prediction of Tunnel Roofs in a Karst Region Based on Catastrophe Theory. *Appl. Sci.* **2025**, *15*, 978. https://doi.org/10.3390/app15020978

1. Introduction

Karst landscapes, defined by features such as sinkholes and caves, cover about 15% of the Earth's surface and are globally distributed [1]. China hosts some of the largest karst systems, particularly in provinces like Guizhou, Guangxi, and Yunnan, where these terrains offer both opportunities and challenges for infrastructure, notably tunnel construction [2]. Current research and field observations indicate that the construction of karst tunnels is notably influenced by factors such as karst caves, the presence of filling materials, and the risks of water and mud inrushes. A common engineering issue encountered in karst areas pertains to the instability and potential collapse of rock formations located between the tunnel and the karst cave. This poses substantial threats to the safety and integrity of tunnel construction and subsequent operations. Consequently, investigating the optimal safe thickness of rock strata between tunnels and karst caves is of considerable practical importance. This research aims to ensure the stability of these rock strata, thereby safeguarding the construction process and operational safety of tunnels in karst areas [3,4].

The stability of tunnels and the safety thickness of dikes in karst areas is a critical issue attracting the attention of numerous researchers. Approaches to address these challenges include empirical methods, numerical simulations, and theoretical calculations.

In empirical research, Zhong et al. [5] reviewed construction experiences across several major Chinese cities, suggesting methods for karst cave pretreatment. Ou et al. [6] assessed rainfall impacts on tunnel water inflow, proposing safety measures for tunnel structures. Yang et al. [7] introduced a novel grouting method for underwater tunnel construction, while Wang et al. [8] developed a semi-empirical model predicting the safety thickness of karst cave roofs. For numerical simulations, Li et al. [9] developed a method to predict hidden karst cave tops via displacement monitoring, while Liu et al. [10] optimized shield velocity to minimize cave disturbance. Fang et al. [11] and Ma et al. [12] explored discrete element models and lattice spring models, analyzing rock stability and failure modes during tunnel excavation. Theoretical research has furthered the understanding of tunnel collapse mechanisms. Yang et al. [13–16] and Zhong and Yang [17] used advanced criteria and theorems to analyze collapse forms and derive analytical solutions. Huang et al. [18] and Yang and Zhang [19] focused on calculating minimum safe thicknesses, while Yang et al. [20] and Liu et al. [21] examined geological disaster impacts and backfill strength deterioration. Li et al. [22] proposed novel stability analysis methods for filled karst caves. Overall, empirical methods, while conservative, often lack precision due to varying geological conditions. Numerical simulations incorporate multiple factors but require practical validation. Theoretical calculations offer a robust foundation, yet their complexity and parameter sensitivity limit practical applicability.

In recent years, the catastrophe theory has been increasingly applied to address the stability issues in geotechnical engineering. This theory determines the critical failure conditions through the principle of total potential energy, facilitating the assessment of structural stability. Qin et al. [23] explored slope sliding instability using the cusp abrupt change theory, developing an instability criterion. Tao et al. [24] integrated landslide case models with abrupt change theory to derive a peak abrupt change model and its inversion method for analyzing the medium and long-term evolution of landslides. Jiang et al. [25] employed the cusp mutation model to study the calculation of safe roof thickness in karst areas, outlining necessary instability conditions for subgrade caves. Yang and Xiao [26] considered the tunnel's shape, span, and depth to formulate expressions for elliptic plate and beam models of critical safety thickness using abrupt change theory. Zhang et al. [27] established a three-dimensional simulation model for tunnel excavation to develop an equation for determining the minimum safe thickness of surrounding rock against water inflow, incorporating sudden change and strength theories. Meanwhile, An et al. [28] applied the cusp abrupt change theory to derive an analytical solution for the safety thickness between buried karst caves and tunnels affected by compressive faults, thereby setting a criterion for the failure of rock slabs in tunnel structures.

According to the analysis presented above, it is apparent that current research on the safety thickness of karst tunnel roofs, grounded in catastrophe theory, primarily focuses on simplified elastic beam and plate models. In most studies, the self-weight is simplified as a uniformly distributed surface force. However, in reality, gravity is a body force related to the thickness of the rock beam. To date, no reports have been found on instability prediction models for tunnel vaults that consider gravity as a body force. Therefore, building on previous achievements, this paper employs catastrophe theory analysis methods, comprehensively considering factors such as gravity and cave distribution to further investigate the safety thickness of tunnel roofs in a karst region, and develop prediction methods for vault instability for the conditions of elastic formulation.

2. Tunnel Roof Rock System Model

2.1. Basic Theories of Cusp Catastrophe Model

The failure of rock formations located between a tunnel and a cave under external loads can be understood as a phenomenon characterized by the dissipation of stored elastic energy [16]. The critical state of this process is associated with a pivotal value of the tunnel vault's displacement. Once the deformation of the vault surpasses this critical displacement, the rock mass tends to become unstable, potentially leading to collapse. The thickness of the rock layer separating the tunnel from the karst cave is identified as the critical safe thickness for the karst tunnel roof. Consequently, modern nonlinear catastrophe theory can be effectively employed to evaluate the safe distance between the tunnel and cave, facilitating the prediction of potential instability.

The fundamental concept of this approach involves predicting the system's response to varying influential variables by formulating diverse differential equations within the system. Presently, the cusp catastrophe model stands as the most prevalently utilized framework for addressing engineering problems in karst regions. This model provides a standard form for the potential function, offering invaluable insights into system behavior and stability [23].

$$V(x) = \frac{1}{4}x^4 + \frac{1}{2}ux^2 + vx \tag{1}$$

where x represents the state variable; u and v denote the control variables

In the context of catastrophe theory, the potential function of the cusp catastrophe model is derived

$$\Delta = 4u^3 + 27v^2 = 0 \tag{2}$$

By integrating Equation (2), it becomes feasible to transition through the bifurcation set when 'u' is less than or equal to zero. The essential criterion for the failure of the rock system corresponds to Equation (3).

$$u \leq 0 \tag{3}$$

When the control variables u and v satisfy both Equations (2) and (3), the entire system is in a state of malfunction. By applying the aforementioned theory, it can be concluded that obtaining the total potential energy of the system is sufficient to estimate the safe state of the tunnel. Figure 1 illustrates the fundamental model of cusp catastrophe theory.

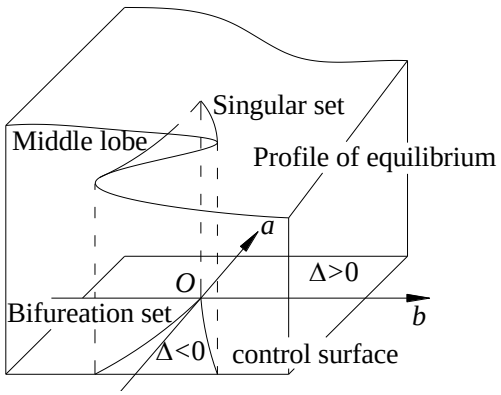

Figure 1. Cusp catastrophe model sketch map.

2.2. Mechanical Model and Reasonable Hypothesis

When the potential function and its branch set equations are established by using the cusp catastrophe theory, a suitable mechanical model needs to be constructed. In the literature [25,26], the strata between the tunnel and karst cave were analyzed as elliptic plates or fixed beams, but the gravity of rock plates was simplified to a uniform surface

load, and the impact of the cave's distribution perspective was overlooked. Therefore, some modifications were needed to establish the mechanical model of the karst tunnel roof as shown in Figure 2. Based on engineering experience and previous research results, specific assumptions are made in the model:

(1) The rock mass system structure of the tunnel roof remains intact without cracks or defects, and the tunnel is parallel to the cave.
(2) The mechanical model of the tunnel roof is regarded as a homogeneous beam with fixed support at both ends, and the geological tectonic stress at both ends of the rock beam is simplified as axial force.
(3) The effect of water on the roof strata of the tunnel is only performed by pressure, and its weakening effect on surrounding rock parameters is ignored.

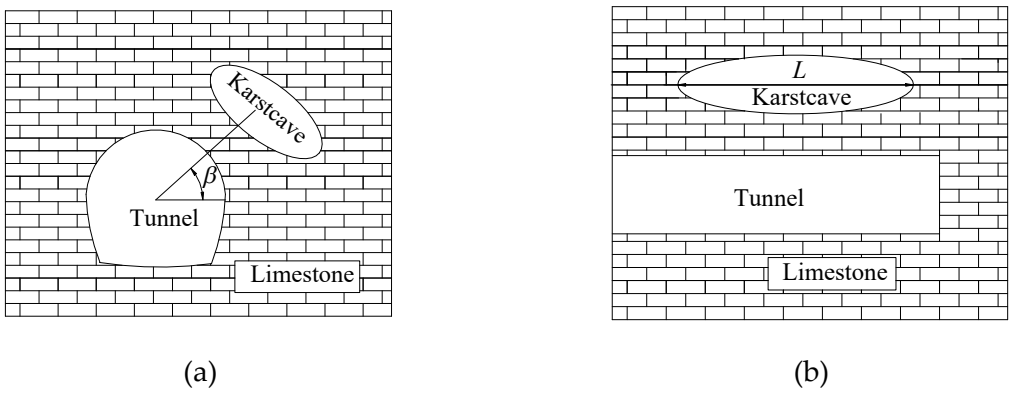

Figure 2. Structure of tunnel proof in karst region: (**a**) View 1 of karst cave position; (**b**) View 2 of karst cave position.

The mechanical model depicted in Figure 3 presents a simplified representation. Here, L denotes the span of the roof, the horizontal width is set as unity, D represents the thickness, E stands for the elastic modulus of the rock, q signifies the dead weight, p symbolizes the simplified cavity pressure, and N indicates the axial force at the rock beam's ends. Additionally, β represents the distribution perspective of karst caves.

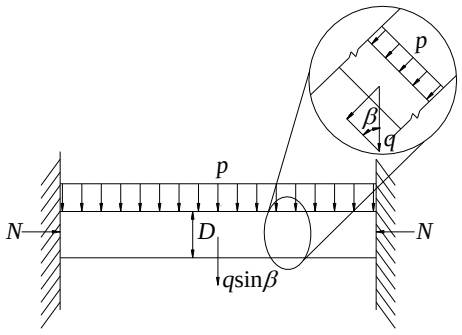

Figure 3. Mechanical model of clamped beam.

3. Analysis of Safety Thickness

The process of rock bending deformation can be viewed as the accumulation of external energy. Instability failure occurs in the tunnel when the elastic energy reaches a critical value. Therefore, the first step is to calculate the total potential energy of the system, construct the potential function expression, transform it into the standard mathematical expression of the sharp point catastrophe model, and then determine the safe thickness of the tunnel roof.

3.1. Potential Function of Rock Systems

Based on the model illustrated in Figure 3, the overall potential energy of the system corresponds to the variation in the beam's strain energy, encompassing bending strain energy, beam potential energy, and alterations in the external force's work performed.

$$U = U_1 + U_2 - U_3 - U_4 \tag{4}$$

where U_1 and U_2 are bending strain energy and potential energy increased by the system, U_3 is the stemming energy from the combined effects of gravity and water pressure, and U_4 results from the action of axial tectonic forces.

According to mechanical analysis, the deflection function of the beam is denoted as $y(x)$

$$y(x) = \frac{w}{2}\left(1 - \cos\frac{2\pi x}{L}\right) \tag{5}$$

where w denotes the deflection at the position $x = L/2$. The deflection is zero at both ends of the beam ($x = 0$ and $x = L$).

Based on the principles of bending theory derived from elasticity and material mechanics, the elastic strain energy function U_1 for the beam can be expressed as:

$$U_1 = \frac{1}{2}\int_0^L M(x)\mathrm{d}\varphi \tag{6}$$

where E represents the elastic modulus of the rock beam, while I denotes the moment of the rock beam; y' and y'' are the first and second derivatives of $u(x)$.

$$\begin{cases} M(x) = EIy'' \\ \mathrm{d}\varphi = \frac{\mathrm{d}s}{\rho} = \frac{M(x)}{EI}\mathrm{d}s \\ \mathrm{d}s = \sqrt{1 + (y')^2}\mathrm{d}x \end{cases} \tag{7}$$

By introducing variables and substituting Equation (7) into Equation (6), then making a Taylor extension for Equation (6), the function of elastic strain energy U_1 is obtained

$$U_1 = \frac{1}{2}\int_0^L EI(y'')^2\mathrm{d}s = \frac{EI\pi^6}{8L^5}w^4 + \frac{EI\pi^4}{L^3}w^2 \tag{8}$$

Similarly, bending strain energy and potential energy increase, as expressed by U_2, work undertaken by gravity and water pressure is expressed as U_3, and work undertaken by axial tectonic force U_4 is calculated.

$$\begin{cases} U_2 = \int_0^L qDy\sin\beta\mathrm{d}x \\ U_3 = \int_0^L (qD\sin\beta + p)(L - x)(y')^2\mathrm{d}x \\ U_4 = \int_0^L N\left(1 - \sqrt{1 - (y')^2}\right)\mathrm{d}x \end{cases} \tag{9}$$

Substituting Equations (8) and (9) into Equation (4), then the simplified function of total potential energy is

$$\begin{aligned} U \quad &= U_1 + U_2 - U_3 - U_4 \\ &= \frac{\pi^2}{4L}\left(\frac{4EI\pi^2}{L^2} - (qD\sin\beta + p)L - N\right)w^2 \\ &+ \frac{EI\pi^6}{8L^5}w^4 - \frac{1}{2}qDL\sin\beta w \end{aligned} \tag{10}$$

3.2. Critical Safety Thickness

To align with the principles of the cusp catastrophe model, we can reformulate Equation (10) as follows:

$$\begin{cases} x = \left(\frac{EI\pi^6}{2L^5}\right)^{\frac{1}{4}} w \\ u = \frac{\pi^2}{2L}\left(\frac{2L^5}{EI\pi^6}\right)^{\frac{1}{2}}\left(\frac{4EI\pi^2}{L^2} - (qD\sin\beta + p)L - N\right) \\ v = -\frac{qDL\sin\beta}{2}\left(\frac{2L^5}{EI\pi^6}\right)^{\frac{1}{4}} \end{cases} \tag{11}$$

The canonical representation of the potential function in the cusp catastrophe model, along with the bifurcation set equation for the rock system cusp catastrophe model, are discussed

$$\begin{cases} V(x) = \frac{1}{4}x^4 + \frac{1}{2}ux^4 + vx \\ \Delta = 4u^3 + 27v^2 \end{cases} \tag{12}$$

Upon analysis, system failure is determined to transpire exclusively when the control variables u and v fulfill the bifurcation set equation. Consequently, the requisite and sufficient criteria for rock system failure are derived:

$$\begin{cases} \left(\frac{4EI\pi^2}{L^2} - (qD\cos\alpha + p)L - N\right)^3 + \frac{27EIq^2D^2\cos^2\alpha}{2} = 0 \\ \frac{4EI\pi^2}{L^2} - (qD\cos\alpha + p)L - N \le 0 \end{cases} \tag{13}$$

In practical engineering applications, when the tunnel is not over-buried, the value of N is usually not large, so it can be considered that the tectonic force N has little influence on the potential function, so the model can be further simplified, and the critical condition for the sudden instability of the karst tunnel system can be obtained as follows:

$$\begin{cases} \left(\frac{4EI\pi^2}{L^2} - (qD\sin\beta + p)L\right)^3 + \frac{27}{2}EIq^2D^2\sin^2\beta = 0 \\ \frac{4EI\pi^2}{L^2} - (qD\sin\beta + p)L \le 0 \end{cases} \tag{14}$$

where the inertia moment of rock beam I is obtained as $I = D^3/12$.

When the structural force N is ignored, further calculation finds that the results of Equations (13) and (14) show no significant difference [26]. Therefore, the critical safe thickness of the karst tunnel roof can be further simplified as:

$$D^3 - \frac{3qL^3\sin\beta}{E\pi^2}D - \frac{3pL^3}{E\pi^2} \le 0 \tag{15}$$

Let $P = \frac{3qL^3\sin\beta}{E\pi^2}$, $Q = -\frac{3pL^3}{E\pi^2}$, and Equation (15) is explained as follows:

$$H^3 + PH + Q \le 0 \tag{16}$$

The equation represented by Equation (16) is used to derive the critical safety thickness expression.

$$D = \sqrt[3]{-\frac{Q}{2} + \sqrt{\frac{Q^2}{4} + \frac{P^3}{27}}} + \sqrt[3]{-\frac{Q}{2} - \sqrt{\frac{Q^2}{4} + \frac{P^3}{27}}} \tag{17}$$

4. Factor Analysis for Safety Thickness

To analyze the stability of tunnel roofs, a parametric analysis is performed to analyze the impact of parameters of interest under karst conditions. For this purpose, numerical

results are obtained and provided in the form of graphs that correspond to $L = 6$ m, $q = 0.2$MPa, $E = 0.2$GPa, $q = 20\text{kN/m}^2$, and $\beta = 90°$. For the value ranges of the relevant parameters, please refer to corresponding engineering case studies [25,29].

4.1. Span Influence

By assuming a calculation span ranging from 2 to 12 m, the relation curve between span (L) and thickness (H) is depicted in Figure 4a. Results indicate a noticeable increase in the critical safety thickness with the expansion of the span, as depicted in the different curves.

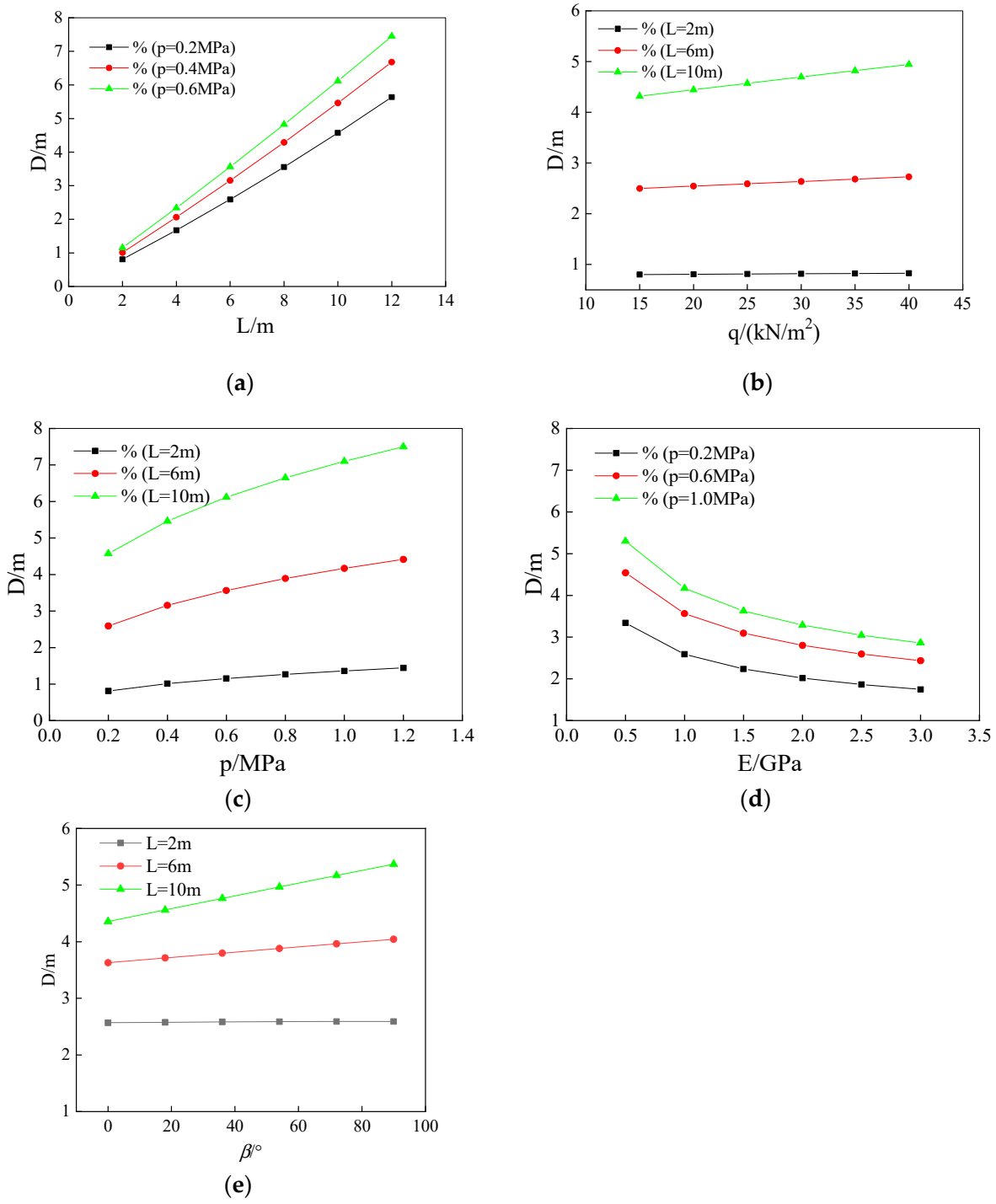

Figure 4. The relationship of safety thickness and factors: (**a**) *D*~*L* relation curve; (**b**) *D*~*p* relation curve; (**c**) *D*~*E* relation curve; (**d**) *D*~*q* relation curve; (**e**) *D*~*β* relation curve.

4.2. Load Influence

When the load (p) varies from 0.2 MPa to 1.2 MPa, the relation curve between load (q) and critical safety thickness (D) is illustrated in Figure 4b. Observations reveal a correlation where critical safety thickness tends to rise gradually with increasing load, particularly evident in scenarios with larger spans.

4.3. Modulus of Elasticity Influence

With the surrounding rock's elastic modulus ranging from 0.2 to 1.2 GPa, based on the research data of limestone rock [26], the critical safe thickness of the roof decreases as pressure within the solution chamber increases. Notably, an actual elastic modulus of around 1 GPa significantly impacts the critical safety thickness, highlighting the substantial influence of surrounding rock mechanical parameter deterioration on tunnel vault stability, as depicted in Figure 4c.

4.4. Rock Gravity Influence

Assuming rock gravity values between 15 and 40 kN/m^3, the relation curve between rock gravity (q) and critical safety thickness (D) is shown in Figure 4d. While a positive correlation exists between roof thickness and rock gravity, the overall weight of the surrounding rock minimally affects safety thickness.

4.5. Distribution Perspective of Cave Influence

Considering the cave's distribution perspective (β) ranging from 0 to 90 degrees, the relation curve between tunnel gradient (q) and critical safety thickness (D) is presented in Figure 4e. The position of the cave significantly impacts the safety thickness, with the most pronounced effect observed at the tunnel crown.

5. Analysis of Engineering Example

In order to enhance the validation of the calculation outcomes and guarantee the safety of the tunnel, the DouMo Tunnel of Shanghai to Kunming high-speed railway and the LuZhuBa tunnel of the Yichang–Wanzhou Railway are taken as examples for application analysis [29], which are located in Anshun, Guizhou Province and Enshi, Hubei Province.

(1) DouMo Tunnel

During the construction of the DouMo Tunnel, a large solution cavity with abundant water and heavy mud was encountered. The measured water pressure ranged from 0.37 to 0.42 MPa, the main strata are limestone and sandstone, with a density of 25 kN/m^3, exhibiting an elastic modulus of 1 GPa, while the rock beam's length connecting the cave and tunnel measured 13 m and the distribution perspective of the cave β was 90°. The separation between the tunnel and the cavern measured 6 m. Due to significant settlement and signs of instability in the tunnel rock beam vault during excavation, curtain grouting was utilized.

(2) LuZhuBa Tunnel

In the LuZhuBa Tunnel, geophysical data indicated the development of karst at DK205+170, posing a risk of disastrous mud protrusion and collapse during construction. The water pressure stabilized at 0.2 MPa after water discharge from the cavity, the main strata are limestone and sandstone, with a density of 23 kN/m^3, the elastic modulus was 0.9 GPa, the length of the rock beams between the caves was 8 m, and the distribution perspective of the cave β was 30°. The precise distance from the revealed tunnel to the concealed cave was approximately 3.6 m, and the tunnel was deemed to be in a secure state.

We integrated these two actual engineering cases into the calculations based on previous research [26], and the novel discoveries disclosed in this manuscript are detailed in Table 1, outlining the summarized outcomes.

Table 1. Comparison of tunnel case calculated by different approaches and the measured data.

Content	Unit	DouMo Tunnel		LuZhuBa Tunnel	
		Research [26]	This Paper	Research [26]	This Paper
Cavity load	MPa	0.4	0.4	0.2	0.2
Rock gravity	KN/m^2	25	25	23	23
Modulus of Elasticity	GPa	1	1	0.9	0.9
Cavity span	m	13	13	8	8
Distribution Perspective of Cave	°	90	90	30	30
Theoretical safe thickness	m	7.30	9.54	5.00	3.56
Actual thickness	m	6	6	3.6	3.6
Theoretical system state	/	collapse	collapse	collapse	stable
Virtual tunnel condition	/	collapse	collapse	stable	stable

6. Instability Predicting and Verification

6.1. Instability Predicting Model

The aforementioned calculation method can judge whether the karst tunnel will eventually become unstable according to the actual state of the karst cave and surrounding rock, but it cannot predict the time of the occurrence of instability. Under specific construction conditions, the tunnel cannot keep a safe distance from the water-rich karst cave when crossing the karst area, so the prediction of the time of tunnel instability becomes particularly important. Thus, corresponding technical measures can be taken before tunnel collapse; as a result, the safety and economy of tunnel construction can be improved significantly.

Furthermore, considering that the parameters of the surrounding rock are difficult to accurately measure in the actual construction environment of a tunnel, and the potential function $V(x) = x^4/4 + ux^4/2 + vx$ is actually a quantity only related to the maximum settlement of the vault, the safety of the tunnel vault can be analyzed by combining the actual monitoring data of the tunnel vault.

Consider the subsidence of tunnel roof as state variable G; the function of state variable changing with time is expressed as follows

$$G = g(t) \tag{18}$$

where t is the accumulated days from tunnel excavation expanding Equation (18) as a Taylor Series; then, taking the first four terms that have a significant effect on the function, the state variable G is obtained:

$$G = g(t) = \sum_{i=1}^{4} m_i t^i \tag{19}$$

where $m_i = \left.\frac{\partial^i f}{\partial t^i}\right|_{t=0}$, let $t = x - Z$, $Z = \frac{m_3}{4m_4}$, Equation (19) can be explained as:

$$\overline{g} = l_4 x^4 + l_2 x^2 + l_1 x + l_0 \tag{20}$$

In Equation (19), the matrix of the coefficients satisfies Equation (20)

$$\begin{Bmatrix} l_0 \\ l_1 \\ l_2 \\ l_4 \end{Bmatrix} = \begin{bmatrix} Z^4 & -Z^3 & Z^2 & -Z & 1 \\ -4Z^3 & 3Z^2 & -2Z & 1 & 0 \\ 6Z^2 & -3Z & 1 & 0 & 0 \\ 1 & 0 & 0 & 0 & 0 \end{bmatrix} \begin{Bmatrix} m_4 \\ m_3 \\ m_2 \\ m_1 \\ m_0 \end{Bmatrix} \tag{21}$$

where l_0 is a constant with no affection to system stabilization, so the state variable G can be converted into the standard form of cusp catastrophe theory:

$$\overline{G} = \frac{1}{4}x^4 + \frac{1}{2}\mu x^2 + vx \tag{22}$$

where $\mu = l_2/2l_4$, $v = l_1/4l_4$.

Similarly, according to the basic theory of cusp mutation, the equilibrium equation of the system and the state standard of system instability can be obtained as Equation (23)

$$\begin{cases} x^3 + \mu x^1 + v = 0 \\ 4\mu^3 + 27v^2 = 0 \\ \overline{G}'' = 3x^2 + \mu < 0 \end{cases} \tag{23}$$

To solve Equation (23), the instability time of the tunnel surrounding rock can be obtained:

$$t = \Delta x \sqrt[4]{1/4l_4} \tag{24}$$

A flow chat for realizing this method is shown in Figure 5.

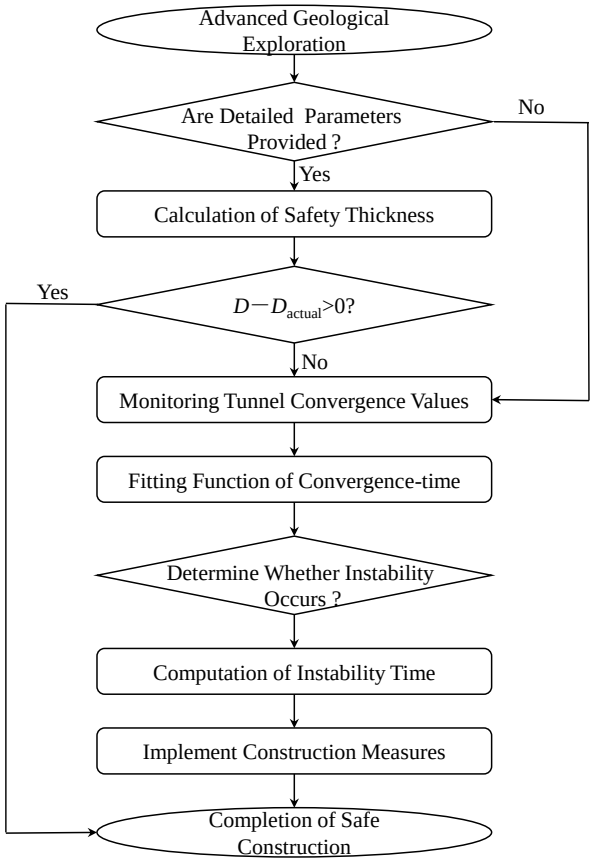

Figure 5. The flow chart of prediction of instability in karst tunnels.

6.2. Practical Engineering Application

Taking a tunnel of the Fangshifang expressway as an example, the instability prediction model of tunnel arch collapse is established based on the actual engineering situation and field-measured data, and the collapse time of the tunnel arch is predicted, and the prediction model of sharp point mutation is tested.

The convergence history curve of the tunnel vault is shown in Figure 6. Through regression analysis, the time history function of the vault settlement of the tunnel can be obtained:

$$g(t) = 1.73 \times 10^{-3}t^4 + 0.02t^3 - 0.51t^2 + 5.74t + 10.20 \quad (25)$$

Substituting the parameters obtained into Equation (20) derives

$$\overline{g} = 1.73 \times 10^{-3}x^4 - 0.55x^2 + 8.26x - 5.91 \quad (26)$$

Substituting the fitted parameters into Equation (20), and performing further standardization according to Equation (21), the following parameters can be obtained: $\mu = -15.98$, $v = 1192.20$. Substituting all parameters into Equations (24) and (25), the result is obtained as $t \approx 24$ d. In the actual tunnel construction process, the tunnel vault collapse occurred 25 days after construction. The comparison demonstrates that the forecasted instability time by the model aligns well with the actual situation, affirming the efficacy of the prediction model derived in this study. This validation offers valuable insights for tunnel design and construction in similar conditions.

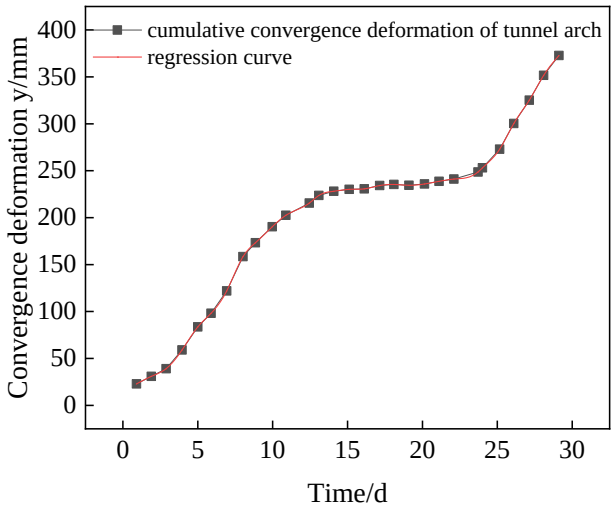

Figure 6. Monitoring cumulative convergence deformation of tunnel arch [29].

7. Conclusions

(1) Through the integration of catastrophe theory and a comprehensive consideration of gravity and cave distribution factors, a discriminant equation for the rock stability of a karst tunnel vault is formulated. The proposed method for calculating roof safety thickness achieves an accuracy improvement of nearly 40% in Case 2. Comparative analyses with existing methods demonstrate that this approach exhibits enhanced accuracy and adaptability, validating its effectiveness for applications in karst tunnel engineering.

(2) Factors such as cave span, the elastic model of surrounding rock, cavity pressure, and cave's distribution significantly impact the safety thickness of the tunnel roof. Specifically, the safe thickness for a 12-m span cave increases by at least 400% compared to a 2-m span. Additionally, for large karst caves (L $\geq$ 10 m), the required safe thickness

at the top is at least 23% greater than that at the sides. These findings emphasize the critical importance of considering the size and location of karst caves to ensure the safety of tunnel construction in karst regions.

(3) A predictive model for the instability time of the karst tunnel vault is established based on empirical data. A case study illustrates a high level of agreement between calculated and observed results, as the error margin is 4%, validating the practicality of the proposed prediction approach.

Author Contributions: Conceptualization, L.P. and Q.T.; methodology, L.P.; software, Y.Z.; validation, Q.T.; formal analysis, Y.Z.; investigation, Q.T.; resources, Y.Z.; data curation, Y.Z.; writing—original draft preparation, Y.Z.; writing—review and editing, Q.T. All authors have read and agreed to the published version of the manuscript.

Funding: This research was funded by the National Natural Science Foundation of China, grant number 51878670, the Innovation-Driven Project of Central South University, grant number 2020zzts163, and the Project supported by the Science and Technology Research Program of Transportation Department of Jiangxi Proyince, China, grant number 2023H0020.

Institutional Review Board Statement: Not applicable.

Informed Consent Statement: Not applicable.

Data Availability Statement: The raw data supporting the conclusions of this article will be made available by the authors on request.

Conflicts of Interest: The authors declare no conflicts of interest.

References

1. Gysel, M. Anhydrite dissolution phenomena: Three case histories of anhydrite karst caused by water tunnel operation. *Rock Mech. Rock Eng.* **2002**, *35*, 1–21. [CrossRef]
2. Zheng, Y.C.; He, S.Y.; Yu, Y.; Zheng, J.Y.; Zhu, Y.; Liu, T. Characteristics, challenges and countermeasures of giant karst cave: A case study of Yujingshan tunnel in high-speed railway. *Tunn. Undergr. Space Technol.* **2021**, *114*, 103988. [CrossRef]
3. Wang, X.L.; Lai, J.X.; He, S.Y.; Garnes, R.S.; Zhang, Y.W. Karst geology and mitigation measures for hazards during metro system construction in Wuhan, China. *Nat. Hazards* **2020**, *103*, 2905–2927. [CrossRef]
4. Lv, Y.X.; Jiang, Y.J.; Hu, W.; Cao, M.; Mao, Y. A review of the effects of tunnel excavation on the hydrology, ecology, and environment in karst areas: Current status, challenges, and perspectives. *J. Hydrol.* **2020**, *586*, 124891. [CrossRef]
5. Zhong, C.P.; Zhu, W.B.; Huang, W.R.; Zhu, S.R.; Xu, M.H. Risk Analysis and Countermeasure Study of Shield Tunnelling in Karst Stratum of China. *Geotech. Eng.* **2019**, *50*, 136–140.
6. Ou, X.F.; Ouyang, L.X.; Zheng, X.C.; Zhang, X.M. Hydrogeological analysis and remediation strategies for water inrush hazards in highway karst tunnels. *Tunn. Undergr. Space Technol.* **2024**, *152*, 105929. [CrossRef]
7. Yang, J.S.; Zhang, C.; Fu, J.; Wang, S.Y.; Ou, X.F.; Xie, Y.P. Pre-grouting reinforcement of underwater karst area for shield tunneling passing through Xiangjiang River in Changsha, China. *Tunn. Undergr. Space Technol.* **2020**, *100*, 103380. [CrossRef]
8. Wang, W.; Gao, S.M.; Liu, L.F.; Wen, W.S.; Li, P.; Chen, J.P. Analysis on the safe distance between shield tunnel through sand stratum and underlying karst cave. *Geosyst. Eng.* **2019**, *22*, 81–90. [CrossRef]
9. Li, S.C.; Wu, J.; Xu, Z.H.; Zhou, L.; Zhang, B. A possible prediction method to determine the top concealed karst cave based on displacement monitoring during tunnel construction. *Bull. Eng. Geol. Environ.* **2019**, *78*, 341–355. [CrossRef]
10. Liu, Z.; Ming, W.H.; Li, J.M.; Zhou, C.Y.; Zhang, L.H. Numerical prediction of the optimal shield tunneling strategy for tunnel construction in karst regions. *PLoS ONE* **2021**, *16*, e0252733. [CrossRef]
11. Fang, Z.D.; Ding, N.; Yang, W.M.; Dai, Z.C.; Wang, J.; He, J.Y.; Ding, R.S.; Ba, X.Z.; Zhou, Z.Q. The Influence of Different Karst Cave Filling Material Strengths on Stratum Stability During Shield Tunneling. *Geotech. Geol. Eng.* **2023**, *41*, 1309–1323. [CrossRef]
12. Ma, J.; Guan, J.; Duan, J.; Huang, L.; Liang, Y. Stability analysis on tunnels with karst caves using the distinct lattice spring model. *Undergr. Space* **2021**, *6*, 469–481. [CrossRef]
13. Yang, X.L.; Huang, F. Collapse mechanism of shallow tunnel based on nonlinear Hoek-Brown failure criterion. *Tunn. Undergr. Space Technol.* **2011**, *26*, 686–691. [CrossRef]
14. Yang, X.L.; Wang, J.M. Ground movement prediction for tunnels using simplified procedure. *Tunn. Undergr. Space Technol.* **2011**, *26*, 462–471. [CrossRef]

15. Yang, X.L.; Yin, J.H. Upper bound solution for ultimate bearing capacity with a modified Hoek-Brown failure criterion. *Int. J. Rock Mech. Min. Sci.* **2005**, *42*, 550–560. [CrossRef]
16. Yang, X.L.; Yin, J.H. Slope stability analysis with nonlinear failure criterion. *J. Eng. Mech.* **2004**, *130*, 267–273. [CrossRef]
17. Zhong, J.H.; Yang, X.L. Kinematic analysis of the three-dimensional stability for tunnel faces by pseudodynamic approach. *Comput. Geotech.* **2020**, *128*, 103802. [CrossRef]
18. Huang, F.; Zhao, L.H.; Ling, T.H.; Yang, X.L. Rock mass collapse mechanism of concealed karst cave beneath deep tunnel. *Int. J. Rock Mech. Min. Sci.* **2017**, *91*, 133–138. [CrossRef]
19. Yang, Z.H.; Zhang, J.H. Minimum safe thickness of rock plug in karst tunnel according to upper bound theorem. *J. Cent. South Univ.* **2016**, *23*, 2346–2353. [CrossRef]
20. Yang, Z.H.; Zhang, R.; Xu, J.S.; Yang, X.L. Energy analysis of rock plug thickness in karst tunnels based on non-associated flow rule and nonlinear failure criterion. *J. Cent. South Univ.* **2017**, *24*, 2940–2950. [CrossRef]
21. Liu, Y.S.; Yang, T.; Zhang, X.; Zhang, Q.S.; Li, X.H.; Liu, J.; Deng, Z.C. Strength deterioration of karst fillings under dry-wet cycles: Testing and modeling study. *Bull. Eng. Geol. Environ.* **2023**, *82*, 339. [CrossRef]
22. Li, S.C.; Lin, P.; Xu, Z.H.; Li, L.P.; He, S.J.; Zhao, S.L.; Huang, X. Innovative Method for the Integral Sliding Stability Analysis of Filling Media in Karst Caves and Its Applications in Engineering. *Int. J. Geomech.* **2017**, *17*, 04017109. [CrossRef]
23. Qin, S.Q.; Jiao, J.J.; Wang, S. A cusp catastrophe model of instability of slip-buckling slope. *Rock Mech. Rock Eng.* **2001**, *34*, 119–134. [CrossRef]
24. Tao, Y.; Cao, J.; Hu, J.M.; Dai, Z.C. A cusp catastrophe model of mid-long-term landslide evolution over low latitude highlands of China. *Geomorphology* **2013**, *187*, 80–85. [CrossRef]
25. Jiang, C.; Zhao, M.H.; Cao, W.G. Stability analysis of subgrade cave roofs in karst region. *J. Cent. South Univ. Technol.* **2008**, *15*, 38–44. [CrossRef]
26. Yang, X.L.; Xiao, H.B. Safety thickness analysis of tunnel floor in karst region based on catastrophe theory. *J. Cent. South Univ.* **2016**, *23*, 2364–2372. [CrossRef]
27. Zhang, L.W.; Fu, H.; Wu, J.; Zhang, X.Y.; Zhao, D.K. Effects of Karst Cave Shape on the Stability and Minimum Safety Thickness of Tunnel Surrounding Rock. *Int. J. Geomech.* **2021**, *21*, 04021150. [CrossRef]
28. An, P.T.; Li, M.X.; Ma, S.K.; Zhang, J.B.; Huang, Z. Analysis of the thickness of the outburst prevention layer in karst tunnels under the control of compressive faults. *Tunn. Undergr. Space Technol.* **2024**, *147*, 13. [CrossRef]
29. Cao, Q. Study on Safe Thickness for Rock Between Tunnel and Karst in Karst Region. Ph.D. Thesis, Beijing Jiaotong University, Beijing, China, 2010. (In Chinese).